Study of the Photon Remnant in Resolved Photoproduction at HERA

Aqsa Ahmed

University College London

Submitted as a final year full unit project

March 23, 2005

Abstract

Photoproduction at HERA is studied in *ep* collisions, with the ZEUS detector, for γp centre-of-mass energies ranging from 130-270GeV. A sample of events with two high-pt jets (pt>6GeV,n<1.6) and a third cluster in the approximate direction of the electron beam is isolated using a clustering algorithm. The third cluster is identified as the photon remnant. Using the actual data values from the paper "*Study of the photon remnant in resolved photoproduction",* a comparison is made with the Monte Carlo data, which was run for 200,000 events with pt=0.0 up to pt=5.0. It was found that the Monte Carlo data best agrees with the paper at pt=1.

Contents:

- **Analysis**
- **Conclusion**

HERA

Fig1:The DESY research centre in the suburbs of Hamburg is home to what is in effect the world's largest electron microscope. HERA (the Hadron-Electron Ring Accelerator) is a unique machine that collides electrons with protons. . This aerial view shows the path of HERA's 6.3 km long tunnel, which extends out from DESY's main site near the bottom centre of the picture, past the horse trotting ring (centre right) and the stadium of the Hamburg football club.

The layout of HERA is shown in fig1. Two separate magnetic systems guide the electron and proton beams around a 6.3Km long ring. DESY and PETRA serve as injectors. There are four interaction regions, two of which are occupied by H1 and ZEUS. A third region has been allocated to HERMES.

HERA DESIGN PARAMETERS

	electron ring		proton ring
circumference		6336m	
energy	30GeV		820GeV
e-p c.m energy		314 GeV	
magnetic bending field	0.164T		4.682T
bending radius of dipoles	610m		534m
circulating current	60mA		160mA
number of particles/beam	0.8X10^13		2.1x10^13
number of bunch buckets	220		220
number of bunches	210		210
current/bunch	0.3 mA		0.8mA
time between beam crossings		96ns	
luminosity		1.5x10^31 cm^-2s^-1	
specific luminosity		3.3x10^29 cm^-2s^-1mA^-2	
polarisation time at Ee=30 GeV	25 min		

Table1: shows some of the parameters of the collider.

HERA, the Hadron-Electron Ring Accelerator was constructed between 1984 and 1990, and measures 6.3km around its circumference. Four separate experiments are located around the ring in four large experimental halls, which are at a depth of around 25 meters. There are two experiments studying collider physics, ZEUS and H1, which are situated at the interaction points where the separate lepton and hadron beams are brought together. Two further experiments, HERMES, which looks at polarization effects, using the lepton beam and a fixed target, and HERA-B, which uses the hadron beam to study CP-violation in B meson decay, are also situated on the HERA ring.

The injection system in HERA works by the injection of electrons and protons in several stages. Protons are accelerated as H- ions in the proton linear accelerator (LINAC) to an energy of 50MeV. These in turn are accelerated to 7.5GeV by the DESY-III proton synchrotron. At this point the electrons are stripped and the protons passed to the PETRA storage ring where they are accelerated to 40GeV. At this energy they are injected into HERA where, guided by super conducting dipole and quadrupole magnets, they are accelerated using conventional radio frequency cavities to the design operating energy of 820GeV. Electrons and positrons are also accelerated by LINACs, first to 220MeV and then 450MeV. They are then transferred to DESY-II for further acceleration to 7.5GeV. From here they go into PETRA where they are accelerated to 12GeV, at which point they are injected into HERA. In HERA the electrons (positrons) are accelerated using conventional and super conducting radio frequency cavities to energies of around 30GeV.

Photon Remnant study

In the study of Photon Remnant in Resolved Photoproduction at HERA the centre of mass energies range from 130-270GeV.

The primary components of this analysis are the calorimeter and the tracking detectors. The uranium-scintillator calorimeter covers 99.7% of the total solid angle. It is subdivided into electromagnetic and hadronic sections with cell sizes 5 x 20 cm^2 and 20 x 20 cm^2. It consists of three parts:

- The rear calorimeter RCAL covering $-3.8 < n < -0.75$
- The barrel calorimeter BCAL covering $-0.75 < n < 1.1$
- The forward calorimeter FCAL covering $1.1 < n < 4.3$

Anatomy of a particle detector

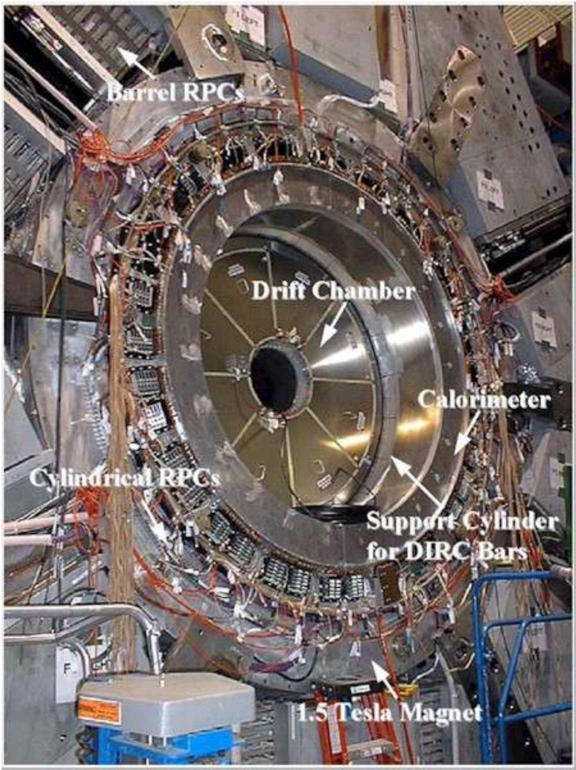

Fig2 shows the different parts of a particle detector.

Calorimeters

Calorimeters are an important class of detectors used for measuring the energy and position of a particle by its total absorption. They differ from most other detectors in that the nature of the particle is changed by the detector. They can also detect neutral as well as charged particles.

Calorimeters are especially important for high energies because of several reasons:

- They can detect neutral particles, by detecting the charged secondaries.
- The adsorption process is statistical, so that the relative precision of energy measurements, ΔE/E varies like E^-1/2 for large E, which is a great improvement on high-energy spectrometers where ΔE/E varies like E^2.
- The signal produced can be very fast, of order 10-100ns, and is ideal for making triggering decisions.

ZEUS Calorimeter

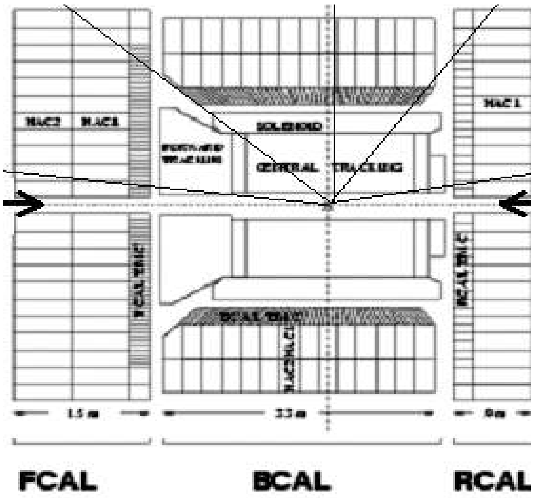

Fig 3: The Uranium-scintillator calorimeter

The Uranium Calorimeter UCAL is the most important part of ZEUS. The primary components used in this analysis are the calorimeter and the tracking detectors. The uranium-scintillator calorimeter covers 99.7% of the total solid angle. It is subdivided into electromagnetic and hadronic sections with cell sizes 5x20 cm^2 and 20x20 cm^2 respectively. It encloses the inner tracking detectors and the solenoid, comprises a cylindrical Barrel Calorimeter BCAL, a Forward Calorimeter FCAL and a Rear Calorimeter RCAL. A Hadron Electron Separator HES is installed between the RCAL layers surrounding the UCAL is the Backing Calorimeter BAC which measures the energy leakage out of the main calorimeter. It contains electromagnetic and hadronic sections in order to have an equal response to both types of energy deposits.

The ZEUS calorimeter is constructed using depleted uranium 238U as an absorber and a plastic scintillator as the readout material. Charged particles transversing the scintilator produce light which travels by internal reflection to wavelength shifters. The light is converted to a longer wavelength by the wavelength shifters and travels to the photo multiplier tubes PMTs at the back of the tower. An electrical signal is produced by these and passed out of the detector. There are two PMTs for each cell. This provides some redundancy and an indication of the x-position of a deposit. Showers initiated by hadrons cannot by described analytically. They may contain both hadronic and electromagnetic components and the relative fractions of these components vary from one shower to another, even if the incident energies are the same. The difficulty arises because some of the energy from the hadronic component goes into nuclear reactions, which are not visible to the scintillator. This means that in general hadronic showers produce less photons in the scintillators than electrons of the same energy. In the uranium, however, the nuclear reactions release high-energy photons, which can be detected in the scintillator. By a suitable choice of thickness for the layers of scintillator and uranium, compensation can be achieved for a very wide range of energies, so that a hadron and electron of the same energy produce, on average, the same number of photons in the scintillator, and hence the signals from the PMTs are the same.

To take advantage of the high resolution achievable by the calorimeter an accurate calibration for all the calorimeter channels must be performed. This is an ongoing process. The principle method is to use the naturally-occurring radiation from the depleted uranium energy is about 2.3MeV, in combination with a point like 60Co source, which can be moved parallel to each scintillator plate’s position.

Tracking system

The tracking system in this analysis consists of a vertex detector and a central tracking chamber inside a 1.43T solenoid magnetic field. The interaction vertex is measured with a resolution along (transverse to) the beam direction of 0.4cm.

ZEUS Detector

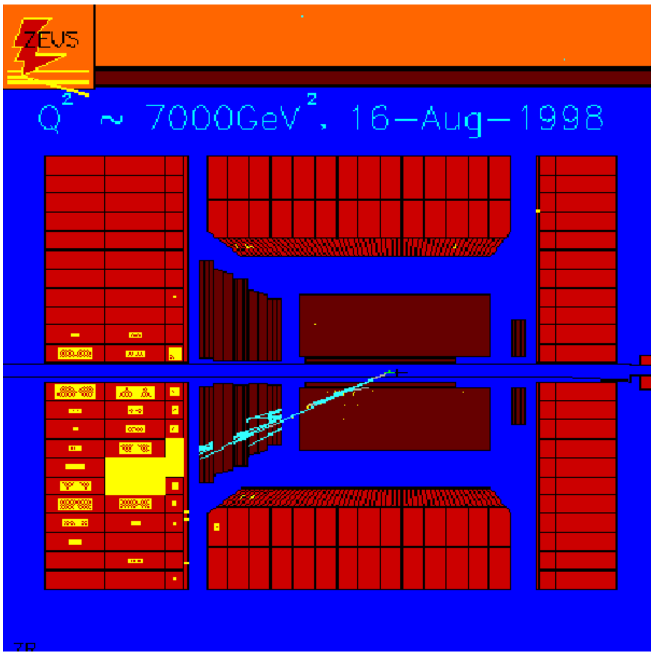

FIG 4: In this side-view of a recent electron-proton collision in the ZEUS detector at HERA, the electron (unseen) has come along central beam pipe from the left, and the proton (also unseen) from the right. The electron has struck a quark in the proton, and this quark has shot out into the detector, converting instantly into a tight spray or "jet" of particles, which leave the tracks pointing to the bottom left-hand corner. The particles then deposit a lot of energy (indicated by the yellow blocks) in the uranium calorimeter, which is specially designed to trap particles like this and measure their energy. The electron, meanwhile, has changed into an electron-neutrino, which leaves no tracks.

ZEUS detector

The ZEUS detector is a multi-purpose magnetic detector, and hermetic apart from a small region close to the beam pipe. The essential elements are a vertex detector (VXD), a central track detector (CTD) plus transition radiation detector (TRD), and planar drift chambers (FTD, RTD) in the field of a thin magnetic solenoid (SOLENOID), an electromagnetic (EMC) and a hadronic calorimeter (HAC) surrounding the coil over the full solid angle, a backing calorimeter (BAC), barrel and rear muon detector (MU), and a forward muon spectrometer (FMU). In addition there are near the beam line photon and electron taggers for the luminosity measurement (fig. 2.1.6), and detector stations for the observation of forward scattered protons. The detector components are laid out in x-y and z-y cross-sections. In the case of the longitudinal cut the proton enters the detector from the right and the positron from the left. A right handed Cartesian coordinate system is used for the ZEUS detector with the z-axis defined as the proton beam direction and the positive y-axis pointing upwards, which means that the x-axis points towards the centre of the HERA ring. The origin is defined at the nominal interaction point. For event analysis a cylindrical polar coordinate system is often used. This has the same z-axis and the azimuthal angle Φ is measured from the x-axis. At HERA the boosts between the lab frame and the more physically motivated frames, such as the centre of mass are in the z-direction. For this reason pseudorapidity $\eta=\ln(\tan(\theta/2$ which is only modified by an additive constant with such boosts is very often used instead of the polar angle θ

At the centre of the detector, closest to the beam pipe and the interaction region is a **Vertex Detector** VXD. This is surrounded radially by the Central Tracking Detector CTD, which is the main component used for tracking charged particles. To the front and the rear of the CTD respectively are the Forward Tracking Detector FTD and the Rear Tracking Detector RTD. In addition a small angle Rear Tracking Detector SRTD was installed to improve the position resolution for charged particles entering the rear calorimeter. Together the inner tracking chambers allow measurement of charged particles emitted from the nominal interaction point at angles between θ =7.5 and θ =170. The tracking detectors operate in a magnetic field of 1.43T, which is provided by a super conducting solenoid. This lies radially between the CTD and the Calorimeter. The VXD is a cylindrical drift chamber with an inner radius of 10.9cm and an outer radius of 15.9cm. it is divided azimuthally into 120 drift cells, each cell occupying 3 degree in azimuth. Each cell has 12 sense and 13 field wires running parallel to the beam. These alternate in a plane extending radially from the beam pipe. On either side of this are planes of 25 drift wires. The entire detector is filled with dimethylether DME gas to provide a slow drift velocity, which gives accurate particle time resolution. The Central Tracking detector CTD of ZEUS is a multiwire proportional chamber, which extends from the VXD to an outer radius of 85cm, and in the z-direction from –100cm to +100cm. The polar angle coverage is 15
< The detector uses 85% Ar, 5%C_2H_6, 10% CO_2.

Luminosity

The luminosity is measured using the electron-proton bremsstrahlung process, by electron and photon lead-scintillator calorimeters installed inside the HERA tunnel.

Two small lead scintillator calorimeters are placed at –34.7m(LUM –e) and –106m (LUM-γ) from the nominal interaction point, which detect photons and electrons respectively. A carbon filter shields the photon calorimeter from synchrotron radiation. These form the luminosity monitors. The primary role of these detectors is to measure the luminosity provided by HERA. They do this using the Bethe-Heitler process ep -> e'pγ where a photon is emitted by the electron at very low angles. The cross section for this process is high. It is observed as signals in both of the luminosity monitors whose energy sum is that of the incoming electron.

Additionally the two monitors serve as tagging devices for collisions occurring at very low Q^2 (photoproduction processes) where the electron is scattered at very low angles, and for initial state bremsstrahlung in neutral current deep inelastic scattering events.

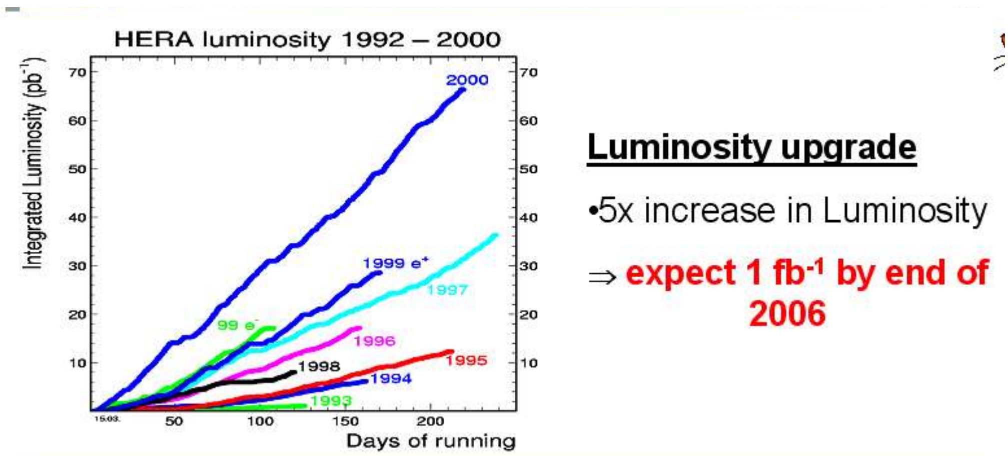

ZEUS Luminosities (pb^{-1})			# events (10^6)
Year	HERA	ZEUS on-tape	Physics
e^-: *93-94, 98-99*	27.37	18.77	32.01
e^+: *94-97, 99-00*	165.87	124.54	147.55

Fig 5: shows the luminosity at HERA from 1992-2000

C5 Counter

The **C5** counter- is attached to the HERA collimator number 5. It consists of a lead plate sandwiched between two scintillator plates within the beam-pipe and is placed perpendicular to the beams. As the collimator particles are passed from the beam halos are registered in the C5 counter and so the arrival time of the bunches are given. This allows a number of useful things to be deduced; in particular the true position of the interaction vertex. In addition to this the counter also measures the rate of interaction produced by the beam, gives information about the beam shapes, and helps to reduce the proton-beam-gas background by vetoing which are not in the time window of a positron-proton interaction. The C5 counter has a time resolution of ~1ns.

The Veto wall - is located near the tunnel exit on the proton beam side of the detector. The main purpose of it is to protect the central detector from the beam halo around the proton bunches. Background particles are absorbed and events arising from particles passing through the veto wall can be rejected. The wall is constructed from iron with two scintillator hodoscopes on each side.

The moun detector – Inorder to detect mouns with energies greater then 2GeV a system of drift chambers divided into forward, barrel, and rear regions was installed

The ZEUS Trigger System

In this analysis**,** photoproduction events are defined by requiring that the electron was scattered at small angles and was not detected in the calorimeter. This requirement corresponds approximately to a cut of Q^2 less then equal to 4GeV^2, giving a median Q^2 of about 10^-3GeV^2. The trigger selects hard scattering events at low Q^2.

Physics events in ZEUS are identified and selected via a 3-tier trigger mechanism. With a bunch crossing occurring every 96ns the trigger must be highly efficient to minimise loss of data and dead time. The data acquisition, DAQ system can only deal with a small fraction of events occurring, however the vast majority of events seen in the detector are non ep interactions, but instead are beam gas interactions caused by beam particles colliding with residual gas in the beam pipes. It is necessary to reduce the rate of events to less than 10MHz but still efficiently select interesting ep events of only ~2-3Hz. Each level of the trigger is more sophisticated than the previous one, requiring more information and time to make a decision on a particular event.

First Level Trigger

The first level trigger, FLT, is purely hardware. Its job is to reduce the rate of data to around 1kHz by eliminating most of the background events. Each component has its own specific FLT and a decision for each event is made by combining the results of each component's decision in the Global First Level Trigger, GFLT. To avoid dead time in the readout system, information from components is stored in pipelines until the decision of the GFLT which occurs at between 4.4 and 5μs after the bunch crossing. The GFLT receives the signal from each component and makes a decision on the event. This is done electronically. The trigger electronics are pipelined as well, with each step repeated every 96ns, so that, as data from one event moves forward one step, data from a new event can enter. At this first stage the trigger information from the calorimeter is the most important factor in deciding the fate of an event.
The CFLT provides information on:

- Total energy of an event
- Tranverse energy of an event
- Missing energy in an event
- Energy and number of isolated leptons
- Electromagnetic and hadronic energy in various regions of the calorimter

The CFLT allows the experimental trigger rate to be kept below 200Hz at the highest luminosities so far experienced at HERA.

In this analysis in the first level trigger the calorimeter cell energies were combined to define regional and global sums which were required to exceed the threshold.

Second Level Trigger

Events which pass the CFLT are passed up the chain to the SLT which is a

Software based trigger. The SLT reduces the rate to around 100Hz by using parallel processing on transputer networks. At this stage, the data is more precise and complete and information coming from different components, which means the data can be correlated. Basic analysis of the information from the components is done by the SLT by looking for signatures of interesting interactions. Information from the first and second level triggers of all events which pass the Global Second Level Trigger, GSLT, are sent to the Event Builder, EVB which combines data from the separate components and merges it into a ZEBRA bank, reformats this into a single event record, according to the ADAMO package, and passes it on to the third level trigger, TLT. Since the time allowed for the decision to be made is much longer than in the FLT, charged particle tracking, better vertex position determination, moun, jet, and scattered electron finding is used in the event decision.

In this analysis the second level trigger mainly rejected beam-gas interactions using timing information from the calorimeter.

Third Level Trigger

The Third Level Trigger, TLT, carries out a more detailed analysis of the information by running a reduced version of the offline analysis software. The input to the TLT consists of a mixture of beam gas, photoproduction and some DIS events. The TLT reduces the rate to 3-5Hz to calculate kinematic properties and perform more refined tracking vertex finding and jet finding. At this stage a geometrical reconstruction is performed for each event. Raw data from the components is corrected using calibration information and information from different events is matched. Events can be classified into particular types depending on what third level triggers they pass.

In this analysis the third level trigger performed further rejections of beam-gas and cosmic ray events using information from both calorimeter and the tracking chambers. An event was rejected if no vertex was found by the central tracking chambers or if the vertex was located in the region lZl > 75 CM. To reject beam- gas interactions, events were selected based on the following kinematic cuts:

- Etot –*pz* > 8GeV
- *pz* /Etot < or = 0.94
- Et*cone* > *or* = 12 GeV

Where Etot, *pz* and Et*cone* are the total energy, the total longitudinal energy and the transverse energy excluding a cone 10^0 cone in the forward direction, respectively. About 470,000 triggers were collected. The following offline cuts were also applied:

- Beam-gas interactions were reduced by tightening calorimeter timing cuts, as well as cuts on the correlation between the vertex position and the calorimeter timing.
- The Etcone cut was raised to Etcone > or = 15 GeV to select hard scattering events.
- To reduce beam-gas interactions, the event was rejected if less than 10% of the tracks pointed toward the vertex.
- Deep inelastic scattering DIS neutral current events were removed.
- The fraction of the initial electron energy carried by the almost real photon, y=Ey/Ee where Ey is the photon energy. The sum runs over calorimeter cells reducing uranium noise.
- To remove charged current background and cosmic ray showers, a cut on the total transverse momentum was imposed.

. **Resolved Photon Interaction**

This is generic label used for all cases in which the photon acts as a source of partons for the hard scatter.

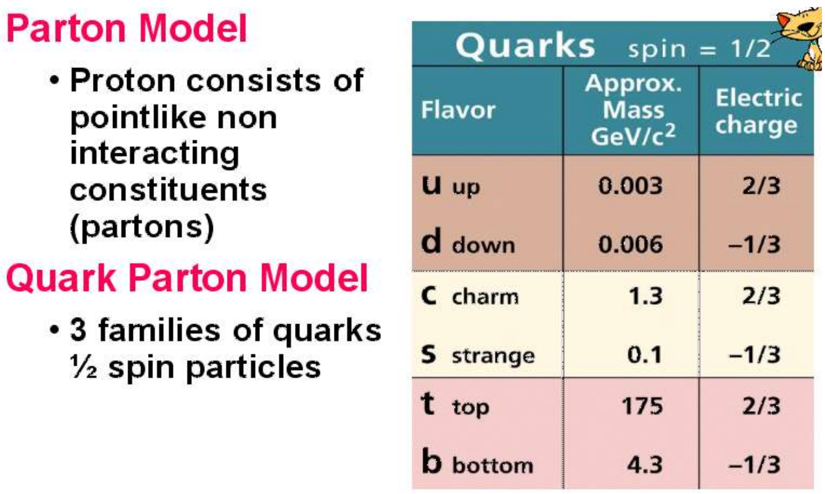

Fig6: Quarks

In resolved photon events there is a photon remnant formed by the partons from the photon which didn't take part in the scatter. The partons in this photon remnant continue in approximately the direction of the incoming photon. In the case of the VMD photon, in the same way as in the proton remnant, the partons have a small intrinsic momentum component *kt* perpendicular to the photon direction *d(sigma)/ dk2t ~ e-bk2t* . For the anomalous photons one expects a harder spectrum *d(sigma)/ dk2t ~ 1/k2t*, due to the *y->qq-* vertex. Experimental evidence for this has been found. As the invariant mass of the quark –antiquark pair produced by the photon rises there will come a point when the transverse momentum of the photon remnant will be the same order as the transverse momentum produced in the hard sub-process. Here there is a continuous transition from anomalous to direct photons, where the highest transverse momentum is produced at the photon vertex.

Jet Algorithms

Since a jet is not a fundamental QCD object it is necessary to find an exact definition. The intention in measuring the jet cross sections is to learn something about the partons from the final hadronic state. However because of QCD confinement it is not possible to 'see' these quarks and gluons directly, but only via the produced hadrons. This leads to the study of properties of the hadronic final state which are: strongly related to the gluons and quarks, experimentally well defined and well measured, and well defined and reliably calculable to all orders in theory. One class of objects that satisfy these conditions is jets.

This definition has a number of unavoidable consequences. There are obviously many ways to define these jets in both theory and experiment. There are however two general constraints on the exact definition of a jet. Firstly it should be independent of a particle splitting into two parallel travelling partons, or in the calorimeter the energy deposit from one particle being split between two cells. In theoretical calculations this would give rise to collinear divergences, which only disappear when no distinction is made between a single particle with energy E', and two collinear particles whose energies sum to the same value ($E_1 + E_2 = E'$), and the contributions from both cases are integrated over. Experimentally this means determining that the results are largely independent of the granularity of the detector. Secondly the result must not be influenced by the emission of very low energy particles. In theory this causes infrared divergences, over which can also be integrated, and in experiment such low energy deposits are considered in connection with detector noise and the cuts used to remove this, which shouldn't affect the result. Algorithms that satisfy these criteria are said to be infrared and collinear safe.

An important question is on what level experiment and theory should be compared. Obviously it would not be sensible to make the comparison on the detector level. On the other hand the hadronisation and shower corrections are not trivial, and decidedly model dependent. Therefore it seems that a comparison on the hadron level is best, since the data is then independent of the physical detector, and from the other side it is as model independent as possible. Hence the cross sections in this analysis were measured on the hadronic level.

For a jet algorithm to be used in photoproduction there are two further demands. For one, the final state, in addition to the partons produced by the hard subprocess, contains the remnant(s) of the incoming hadron (and photon for resolved processes). Any remnant should be separated from the jets, and minimally influence the jet finding. The algorithm should therefore either restrict the size of the jets or handle the hadron remnant as a separate object. Also, for a photoproduction event the laboratory frame in general not the same as any of the physically motivated system such as the photon-proton centre of the mass or the partonic centre of mass. A transformation into any of these would involve a nontrivial measurement. However all these systems have the property that they are boosted in the direction of the beam with respect in the lab. Therefore the jet algorithm should be independent of such boosts as possible. This is automatically achieved when only transverse energy, ET, is considered for jet finding in a plane of pseudorapidity, η, and azimuth, ø. While ET and ø are unaffected by a boost in the beam direction, η alone is shifted by an additive constant. So the form of the transverse energy distribution in η – ø is the same in all frames.

EUCELL

EUCELL uses preclustering. The clusters are however determined by using a grid in the η-ø plane. The size of the cells that make up the grid is determined such that Δηgridcell ≈ Δøgridcell ≈ R/2. preclusters are then found by sliding 3 x 3 cell window over the grid. If the total summed transverse energy of any 3 x 3 section is above a certain level (1 GeV for this analysis) it is counted as precluster. About the centre of each precluster is placed a cone of radius R, then an iterative process is performed until the sets of included objects is stable. The cone with the highest transverse energy, independent of which preclusters it comes from, is accepted as a jet. The enclosed objects that make up this jet are excluded from further jet finding. The whole procedure is repeated again and again until there are no cones with energy above the predetermined threshold. In this way EUCELL produces no overlapping jets. Every object is associated to a jet such that the highest ET in that part of the η-ø plane is produced. In actual fact it is possible that the two jets cones may overlap, but all the energy in the overlap will be associated with the highest ET jet. This situation occurs so rarely, and the jets overlap to such a small extent that it is insignificant, especially considering the resolution of measured ηjet.

Cluster Algorithms

Cluster algorithms are well known from e+e- experiments. Their application to photoproduction was until recently opposed by the fact that they do not treat the beam direction differently to any other, and the separation of the jets from hadron remnants is difficult. These disadvantages are avoided in newer variations. For this analysis the KTCLUS algorithm was used.

Hard Photproduction in ZEUS

In photoproduction at HERA, where the centre of mass energy is much higher than earlier experiments, one expects contributions from direct and resolved photons. In events with resolved photons there is photon remnant, and with direct processes the entire photon energy enters the hard sub process. As already mentioned, the experimental definition of photoproduction at ZEUS is the absence of a scattering positron in the uranium calorimeter, which corresponds to a positron scattering angle of ø e > 176.5° and photons of Q2 < 4GeV2. Hard photoproduction interaction are defined by demanding 'large' values of transverse energy in the final hadronic state *yp* -> *X*, such that a scale is reached at which the internal structure of the photon and proton can be resolved. Any photoproduction event that contains jet satisfies this criterion.

In this analysis only dijet hard photoproduction interactions are considered; that is events 2 or more jets EjetT ≥ 6GeV. The expected event topology consists of a certain number of particles with high transverse momenta, a proton remnant, and in the case of resolved photon processes, a photon remnant.

Monte Carlo

Monte Carlo programs use the parton distribution functions, and the cross section for the hard sub process to generate individual events. Some of them take the out going partons and use parton shower and hadronisation models to produce events as they are in experiment. By treating these generated events in an equivalent way to the date from the detector it is possible to come up with predictions for the measured cross sections. As well as providing predictions, Monte Carlo programs can offer a way to study, and correct for detector effects in the measurement.

Some Monte Carlo programs serve purely to calculate cross sections. These generators produce events with a final state containing the two or three outgoing partons from the hard sub process. The events are then given weights corresponding to the calculated probability of their occurrence, some of which may be negative. After this equivalent cuts are made as for the date, and the events are binned to provide a prediction of the measured cross sections.

Monte Carlo programes and simulated event samples are also needed to study experimental effects on the measurements made using the real data, and to extract a detector independent cross section. For a Monte Carlo event sample to be of any use in this respect is necessary that generator produces events as they appear in the data. There are basically two types of experimental effect that can be dealt with using such Monte Carlo. Firstly correcting for the efficiency and purity with events can be selected. Secondly there is the correction of measured quantities

.

HERWIG

The HERWIG (Hadron Emission Reactions With Interfering Gluons) generator attempts to provide as complete an implementation of the LO p QCD as possible. Non-perturbative effects are described using the simplest possible universal model. The aim is to describe the largest possible number of processes with the fewest possible free parameters, and thereby to have a large predictive power.

For resolved events HERWIG starts by generating the radiated photon from the incoming electron. The next step is to produce the hard subprocess using the LO QCD matrix element for the 2 $\rightarrow$ 3 body scatter.

Absolute Normalisation of the Monte Carlo

Monte Carlo contains a series of approximations, which influence the prediction of the cross section. The most important is that it only considers the hard sub process at LO. This means that the result is highly dependent on the factorisation scale chosen. Also HERWIG uses the two loop calculations for αs the strong coupling constant. In a LO QCD calculation simply changing from a one to a two-loop calculation αs introduces a difference of a factor 1.3. In addition the choice of QCD used in Monte Carlo is complicated by the fact that, as a rule, the parameterisations of the photon and proton structure functions are determined with different values of QCD.

For the most parts these lead to a constant factor (K) in the cross section. Therefore it seems justified to vary the absolute normalisation of Monte Carlo, and if necessary the predicted cross-section.

Detector Simulation

HERWIG and PYTHIA produce final states similar to those produced from beam interactions in the experiment. How this final state will look in the ZEUS detector is found using the program MOZART, which is based on the GEANT package. MOZART simulates the interactions of the final state particles with the various detector components using certain simplifying assumptions. Thus the Monte Carlo final state is converted into the same form as the genuine data, and can be put through exactly the same analysis.

Monte Carlo Sample Used

In this analysis the HERWIG event generator was used to check the PYTHIA results. The cut on the minimum Ptmin, of a hard scatter was set at 2.5GeV. the parton densities used were GRV LO [21] for the photon and MRSD [22] for the proton. For comparison, we also used the parameterization LAC1 [23] for the photon.

Photoproduction Revisited

THE THEORY that describes strong interactions in the standard model is called quantum chromo dynamics or QCD.

It is useful to consider the scatter from the very low Q2 interaction of photo production in two parts. The radiation of the photon, and then, the photon interaction with a parton in the proton. The radiation of the virtual photons from the incoming electrons is an elementary QED (the quantum electrodynamics) process and can therefore be calculated with no further assumptions. The electron beam can then be regarded as a source for mass less quasi-real photons (q2 Ξ p$y \approx 0$) emitted collinear to the beam line. Thus the ep cross section can be expressed in terms of a photon flux *fey(y)* and the cross section for virtual photon proton scattering.

The high c.m. energy of HERA allows the study of photoproduction over a wide energy range.

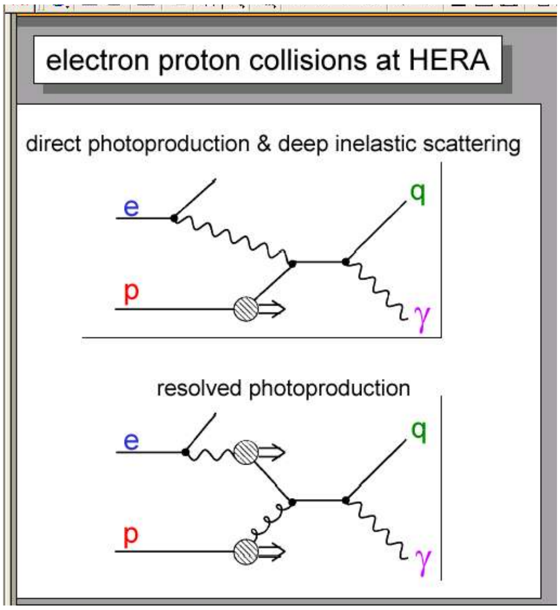

.

Fig7: shows the electron proton collisions at HERA.

With purely hadronic reactions at HERA, photoproduction is expected to have a soft component and a hard component arising from the scattering of a parton from the proton on a parton from a vector meson. However, in addition to its hadronic features, the photon possesses a property, which makes it distinctly different from hadrons: it can couple directly to quarks and the coupling is point like. This leads to additional hard scattering processes which become prominent at high energies and which are not present in hadron-hadron interactions. Two types of diagrams represent them: the first (the direct photon process) result from photon gluon fusion into quark-antiquark Fig8a and from photon scattering off a quark in the proton under the emission of a gluon (QCD Compton process). Together with the hard scattering of the hadronic photon and the hard scattering due to the quark and gluon content of the photon constitute the resolved photon process Fig8b.

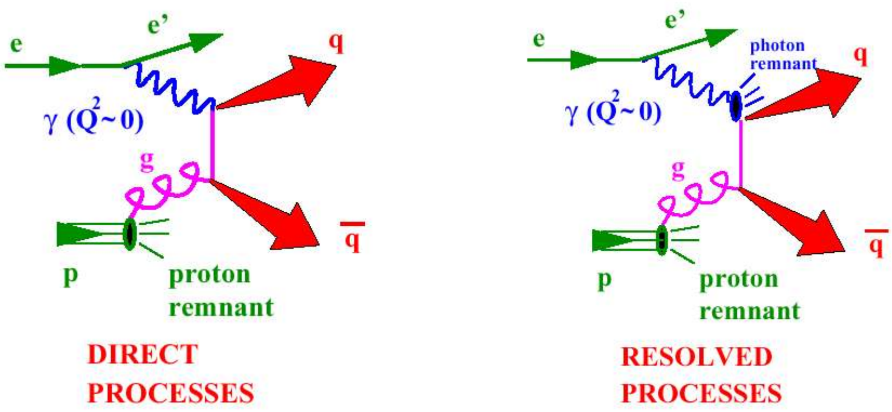

Fig8 :a)Direct and b) resolved processes

In direct processes the final state consists of the two parton jets, the scattered electron close to the electron beam and the proton remnant close to the proton beam. For resolved processes there is in addition the photon remnant which is emitted in the direction of the incident of the incident photon Fig9.

.

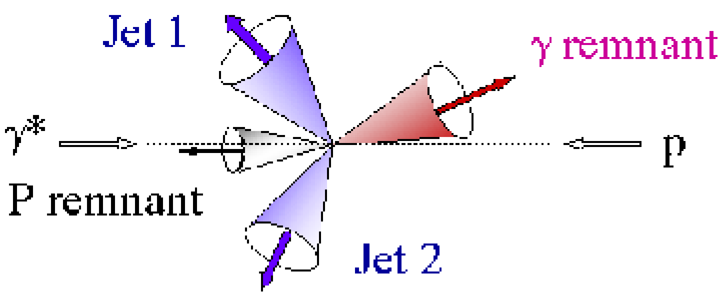

Fig9 :Photon remnant.

The direct and resolved contributions show quite different distributions: in the resolved case only a fraction of the photons momentum participates in the hard scatter such that the centre of mass is more strongly boosted in the proton direction. The data require substantial contributions from resolved processes.

Photon remnant Identification

Since the photon remnant is expected to have low transverse momentum with respect to the beam axis, the separation between the photon remnant and the two jets from the hard scatter can be achieved, by associating the photon remnant with the cluster having the smallest transverse momentum.

Correction procedure

For the Monte Carlo events the Kt algorithm is applied independently at both the generated hadron level and the calorimeter cell level. In both cases the resulting clusters are sorted according to pt. The detector level cuts in ncal,ptcal.E3cal and yjb correspond approximately to two hadron jets with pt1,2>6GeV and n1,2, a remnant cluster with n3<-1 and E3>2GeV, and 0.2<y<0.85.

Analysis

The subroutine (appendix A) was run over 200,000 events for the following values of PT.

PT
0.0
0.1
0.2
0.3
0.4
0.5
0.6
0.7
0.8
0.9
1.0

2.0
3.0
4.0
5.0

Table 2: Values of PT

This Monte Carlo data was compared to the actual data taken by the paper (appendix B). by looking at the following histograms it was found that the simulated events match very closely to the actual data at pt=1

Pt=0

•The rapidity distribution agrees more with the simulated data in the positive region.
•For the transverse momentum distribution (rapcut3= -1 applied) the distribution peaks at 1.5GeV with a tail extending to 6GeV.
•The energy distribution peaks around 7GeV and extends to 20GeV.

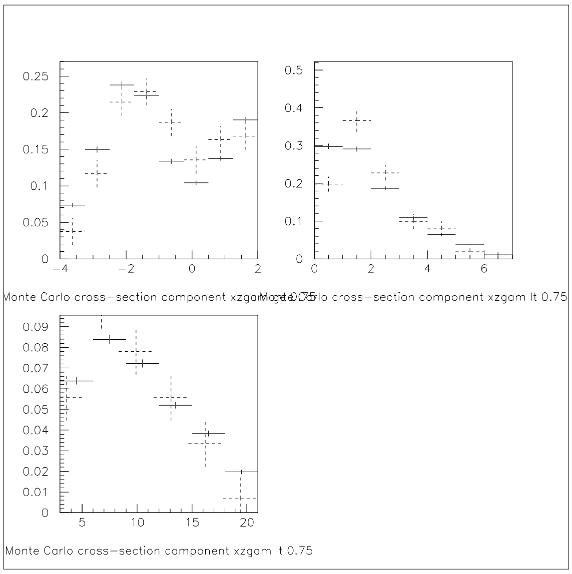

Pt=0.1

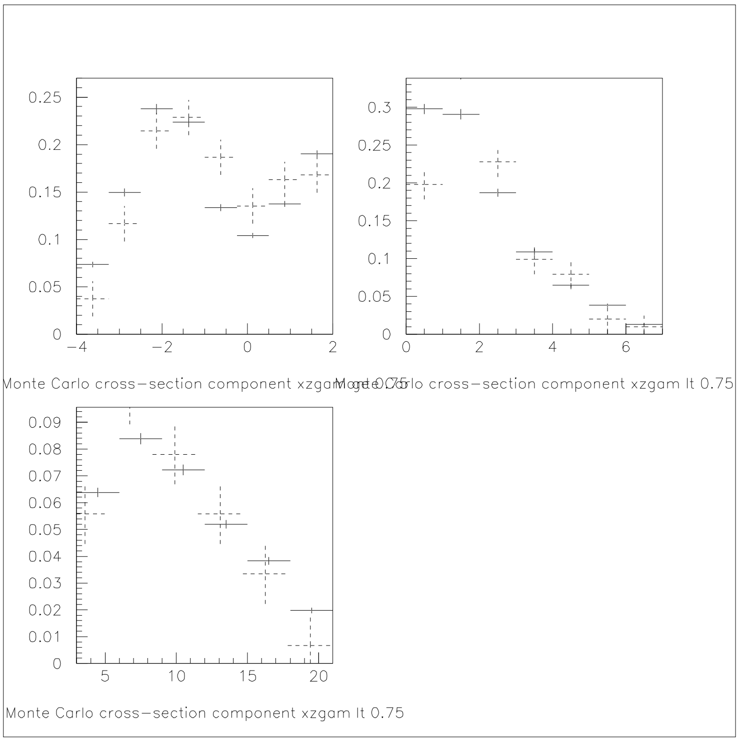
Monte Carlo cross−section component xzgam lt 0.75
Monte Carlo cross−section component xzgam lt 0.75
Monte Carlo cross−section component xzgam lt 0.75

pt=0.2

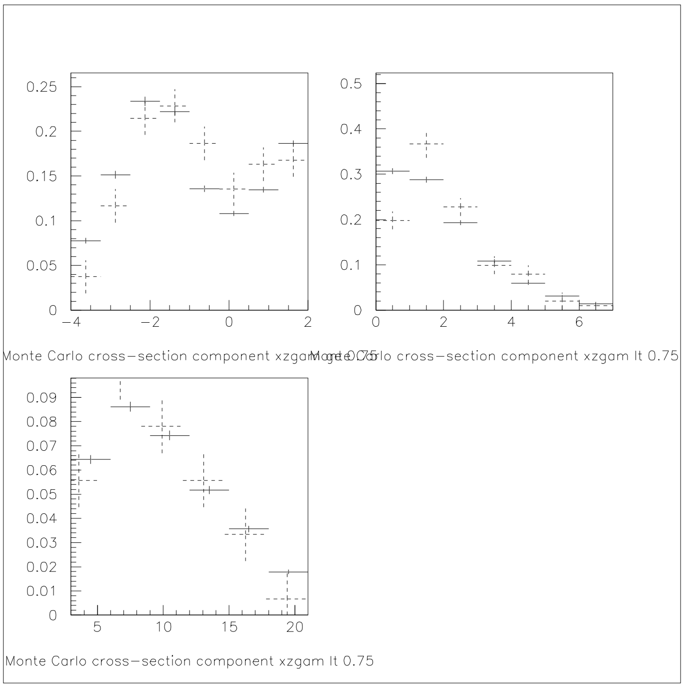
Monte Carlo cross−section component xzgam lt 0.75
Monte Carlo cross−section component xzgam lt 0.75
Monte Carlo cross−section component xzgam lt 0.75

Pt=0.3

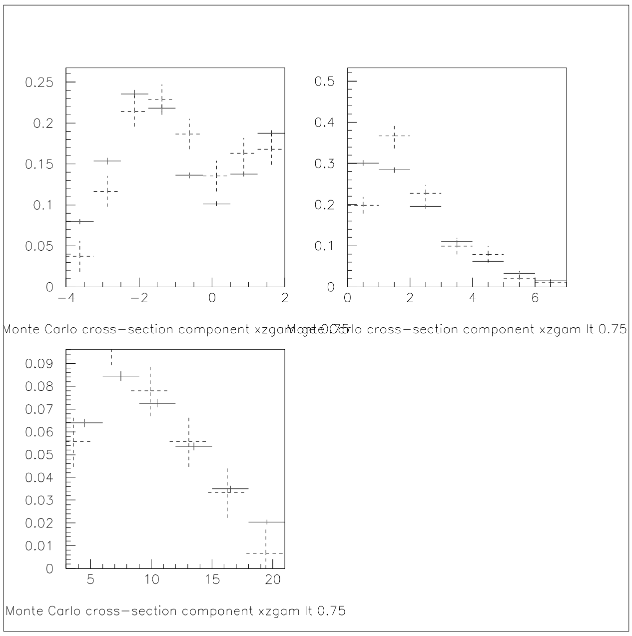
Monte Carlo cross-section component xzgam lt 0.75
Monte Carlo cross-section component xzgam lt 0.75

pt=0.4

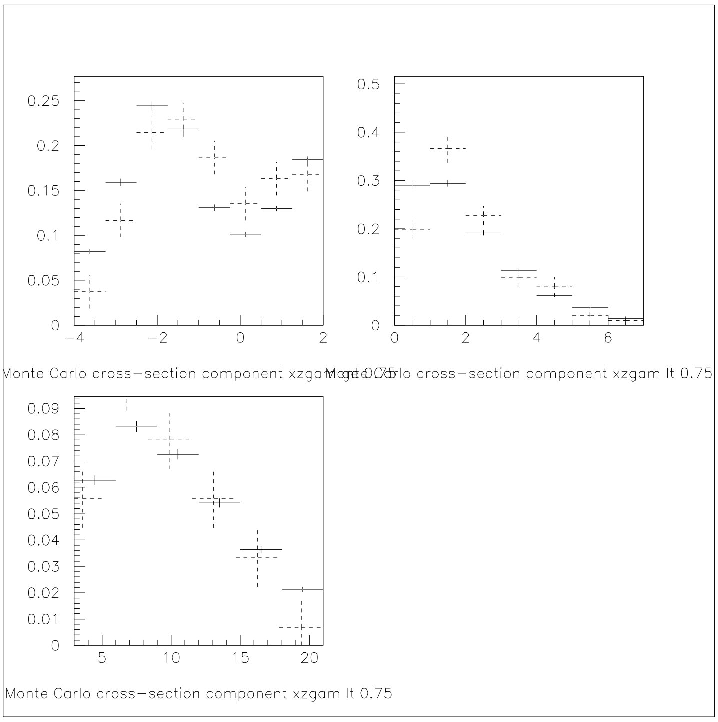
Monte Carlo cross-section component xzgam lt 0.75
Monte Carlo cross-section component xzgam lt 0.75

Pt=0.5

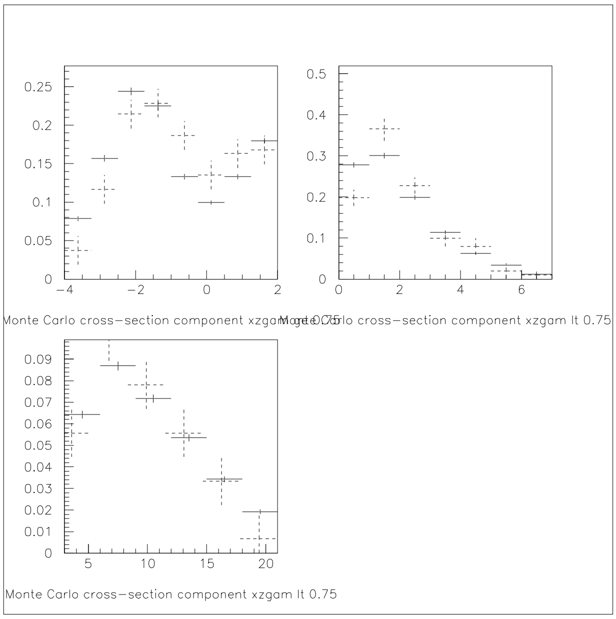

Monte Carlo cross−section component xzgam gt 0.75
Monte Carlo cross−section component xzgam lt 0.75
Monte Carlo cross−section component xzgam lt 0.75

pt=0.6

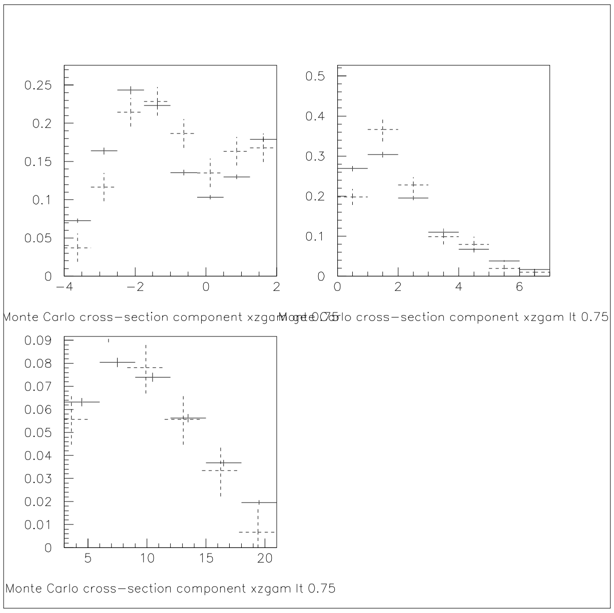

Monte Carlo cross−section component xzgam gt 0.75
Monte Carlo cross−section component xzgam lt 0.75
Monte Carlo cross−section component xzgam lt 0.75

Pt=0.7

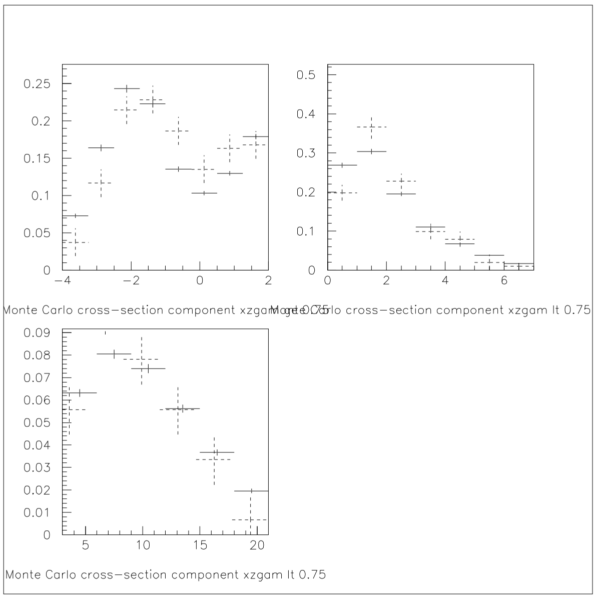
Monte Carlo cross−section component xzgam gt 0.75
Monte Carlo cross−section component xzgam lt 0.75
Monte Carlo cross−section component xzgam lt 0.75

pt=0.8

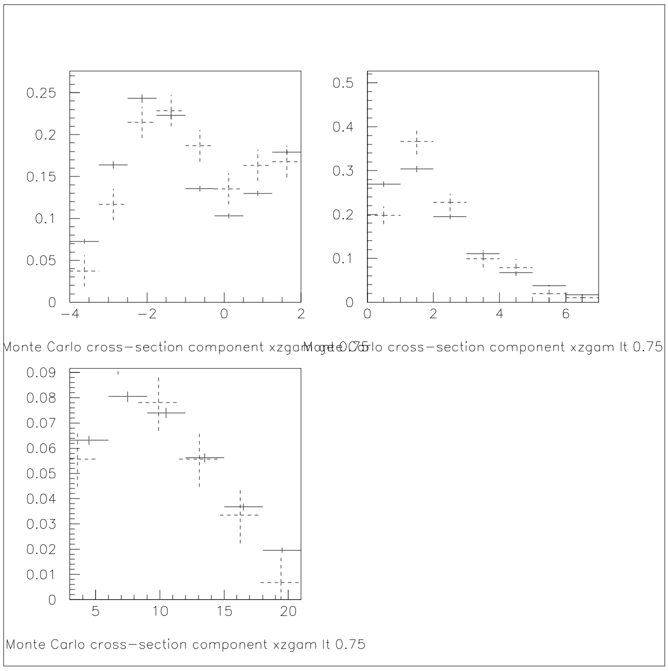
Monte Carlo cross−section component xzgam gt 0.75
Monte Carlo cross−section component xzgam lt 0.75
Monte Carlo cross−section component xzgam lt 0.75

Pt=0.9

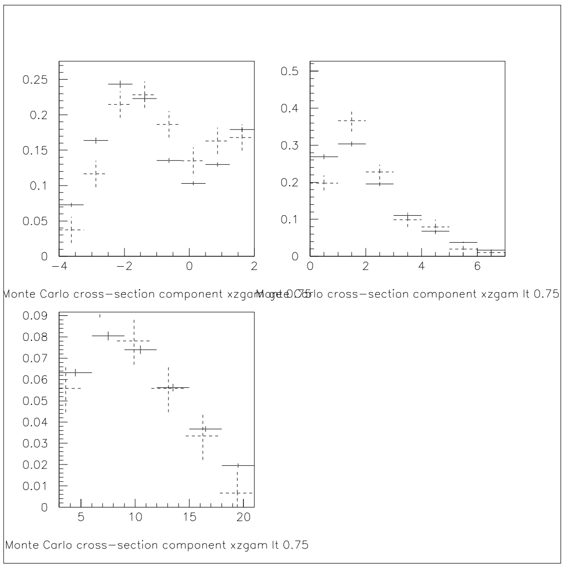

pt =1

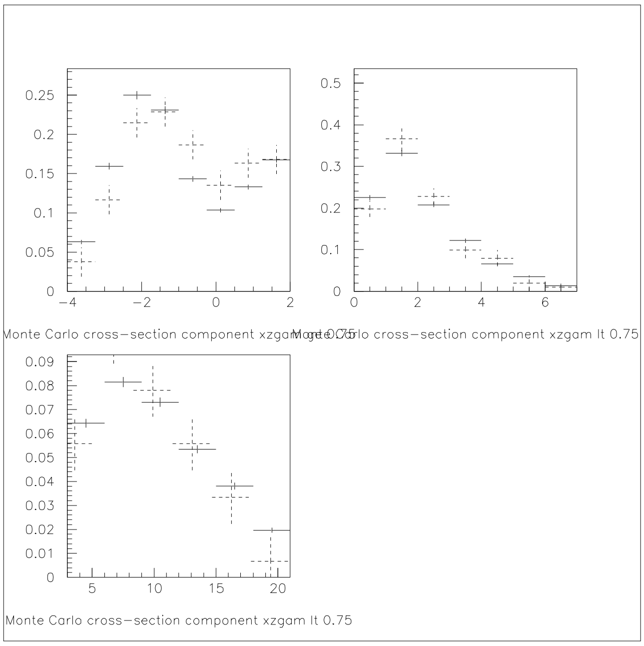

At pt=1 the predictions agree to the theory, as the predicted values are with in the error bars of the actual data. Above pt=1 the prediction values start to go above and shift to the right of the actual data therefore are not use full.

The simulated data for all three graphs seem to agree the most with the actual data at pt = 1.

Pt=2

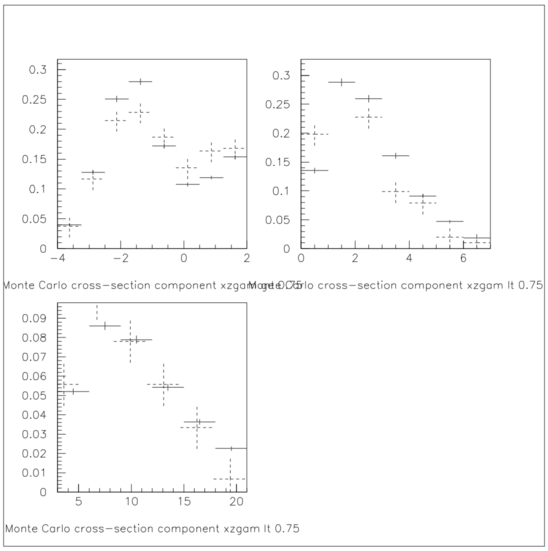

pt=3

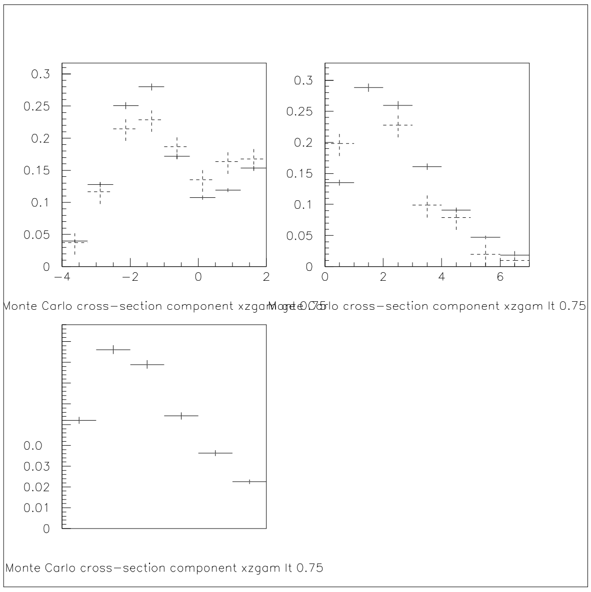

For pt >2 the Monte Carlo data shifts further away from the actual data therefore its of no use to this analysis.

Conclusion

In a sample of quasi-real photon-proton collisions, the photon remnant produced in resolved photon interactions has been isolated . the selected events contain two high – pT jets with pT > 6 GeV and η < 1.6, and 130 < W*yp* < 270 GeV. The properties of the photon remnant, as defined by the cluster with η3< -1 and E3 < 2 GeV, are studied and shown to exhibit a collimated energy flow with a limited transverse energy with respect to the cluster axis, characteristic of a jet structure. The theory best matched while the pt was set at 1. These results are in qualitative agreement with theoretical expectations of the substantial mean transverse momenta for the photon remnant. Several studies have suggested that next to leading order contributions or fluctuations of the photon into quark-antiquark pairs with high virtuality may lead to a 'photon remnant' which has sizable transverse momentum with respect to the incident photon direction

The theory best matched while the pt was set at 1. These results are in qualitative agreement with theoretical expectations of the substantial mean transverse momenta for the photon remnant.